MEDICAL SCIENCE MONITOR

LAB/IN VITRO RESEARCH

e-ISSN 1643-3750
© Med Sci Monit, 2018; 24: 1282-1294
DOI: 10.12659/MSM.906266

Received: 2017.07.18
Accepted: 2017.08.17
Published: 2018.03.03

Src Promotes Metastasis of Human Non-Small Cell Lung Cancer Cells through Fn14-Mediated NF-κB Signaling

Authors' Contribution:
Study Design A
Data Collection B
Statistical Analysis C
Data Interpretation D
Manuscript Preparation E
Literature Search F
Funds Collection G

ABCDEF 1,2 Wei Wang*
ABCDEF 3 Feiyu Liu*
BC 2 Chaoyang Wang
CD 2 Chengde Wang
D 2 Yijun Tang
AE 1 Zhongmin Jiang

1 Department of Thoracic Surgery, Shandong Provincial Qianfoshan Hospital, Shandong University, Jinan, Shandong, P.R. China
2 Department of Thoracic Surgery, Yantai Yuhuangding Hospital, Qingdao University, Yantai, Shandong, P.R. China
3 Department of Pharmacy, Yantai Yuhuangding Hospital, Qingdao University, Yantai, Shandong, P.R. China

* Wei Wang and Feiyu Liu contributed equally to this study

Corresponding Author: Zhongmin Jiang, e-mail: qyjiangzhongmin@sina.com
Source of support: Departmental sources

Background: Src and Fn14 are implicated in the aggressiveness of non-small cell lung cancer (NSCLC) cells, yet the molecular mechanism is not fully understood.

Material/Methods: The proliferation, migration, and invasion of HCC827 cells with *Src* knockdown were examined *in vitro*. The expression of Fn14 and the activation of NF-κB signaling pathway in *Src*-silenced HCC827 cells were detected by western blot. The role of Fn14 in Src-regulated cell migration/invasion and activation of NF-κB signaling was investigated by overexpressing Fn14 in *Src* knockdown NSCLC cells. Furthermore, the pro-metastatic role of Src was validated in a NSCLC metastasis mouse model.

Results: Knockdown of *Src* inhibited the proliferation, migration, and invasion of HCC827 cells, which was associated with reduced levels of Fn14, p-IκBα, p-IKKβ, and nuclear NF-κB p65. Overexpression of Fn14 restored the potential of migration and invasion as well as the activation of NF-κB signaling in *Src*-silenced NSCLC cells. In addition, silencing of *Src* suppressed lung metastasis of HCC827 cells in mice, and inhibited the expression of Fn14 and nuclear translocation of NF-κB p65 *in vivo*.

Conclusions: The data demonstrated that the Src/Fn14/NF-κB axis plays a critical role in NSCLC metastasis.

MeSH Keywords: Carcinoma, Non-Small-Cell Lung • Receptor Activator of Nuclear Factor-kappa B • src-Family Kinases

Full-text PDF: https://www.medscimonit.com/abstract/index/idArt/906266

Indexed in: [Current Contents/Clinical Medicine] [SCI Expanded] [ISI Alerting System] [ISI Journals Master List] [Index Medicus/MEDLINE] [EMBASE/Excerpta Medica] [Chemical Abstracts/CAS]

Background

Lung carcinoma is one of the leading malignancies worldwide. According to global cancer statistics in 2011, lung carcinoma ranked the first among all cancer types in males, and it accounted for 17% of the total of new cancer cases and 23% of the total cancer-related deaths [1–3]. Moreover, the incidence of lung carcinoma in women continues to increase in recent years, and lung carcinoma has become the second most commonly recognized cancer type [1]. The oncogenesis of lung cancer can be triggered by indoor/outdoor air pollution and exposure to occupational or environmental carcinogens. According to histology and cancer genetics, lung carcinoma is normally classified into two major types: non-small cell lung cancer (NSCLC) and small cell lung cancer (SCLC) [4]. Of these two types, NSCLC is diagnosed in approximately 85% of all lung carcinoma cases, and it can be further classified as adenocarcinomas, squamous cell carcinomas, and large cell carcinomas [4]. Currently, chemotherapy remains the standard therapeutic modality for advanced or metastatic NSCLC. However, the response rate is lower than 35% as front-line treatment and is even lower as a second-line option [5–7]. Therefore, it is critical to identify novel biological targets that are associated with oncogenesis and metastasis of NSCLC for the development of effective therapeutic strategies, in order to improve outcomes and survival of NSCLC patients.

Src has been implicated in the progression of NSCLC and other cancers, and several Src inhibitors are at the pre-clinical stage or in clinical trials [8]. Src kinase is a member of the Src family of kinases that are involved in the modulation of diverse cellular signal transductions [9]. Src is a tyrosine kinase that plays critical roles in tumor growth, metastasis, and angiogenesis, and thus it is recognized as a promising therapeutic target for various solid tumors [10,11]. Regarding NSCLC, upregulation of Src kinase is frequently detected, especially in active smokers with squamous cell lung carcinoma [8,12]: elevated expression of Src is observed in 60–80% of adenocarcinomas and bronchioloalveolar cancers and in 50% of squamous cell carcinomas. Cheng et al. found that the positive effect of Src on NSCLC cell invasion was mediated by Fn14, a member of the tumor necrosis factor superfamily of cell surface receptors [13]. Additionally, Src-regulated NF-κB signaling has been demonstrated in various cancers [14,15]. Given the fact that Fn14 regulates the growth of NSCLC and SCLC cells via NF-κB signaling [15,16], we speculated that Src may activate NF-κB signaling via Fn14 in NSCLC cells.

To verify our hypothesis, the regulatory role of Src in the expression Fn14 and the activation of NF-κB signaling in NSCLC cells were investigated by a series of *in vitro* and *in vivo* experiments. NSCLC cell line HCC827 with high expression levels of Src and Fn14 was selected as the *in vitro* cell model and for the *in vivo* metastasis assay. The effect of *Src* knockdown on the proliferation, migration, and invasion of HCC827 cells were assessed. Moreover, the expression of Fn14 and the activation of NF-κB signaling in *Src*-silenced cells were determined. The Src/Fn14/NF-κB axis was further confirmed by the rescue effect of Fn14 overexpression in *Src*-silenced HCC827 and A549 cells. In addition, the Src/Fn14/NF-κB axis in NSCLC cell metastasis was validated in a mouse metastasis model.

Material and Methods

Antibodies and reagents

Antibodies against Fn14 (D121267) and Src (D120536) were purchased from Sango Biotech (Shanghai, China). Antibodies against IκBα (bs-1287R), phosphorylated IκBα (p-IκBα) (bs-18129R), IKKβ (bs-4880R), p-IKKβ (bs-3233R), and Histone H3 (bs-17422R) were purchased from Bioss (Beijing, China). Antibody against nuclear NF-κB p65 (PB0073) was purchased from Boster (Wuhan, China). Antibody against NF-κB p65 (10745-1-AP) used for immunofluorescent staining was purchased from Proteintech (China). Secondary goat anti-rabbit IgG-HRP (A0208), goat anti-mouse IgG-HRP (A0216), and cy3-labled goat anti-mouse IgG (A0521) antibodies were purchased from Beyotime (Shanghai, China). Antibody against β-actin (sc-47778) was purchased from Santa Cruz (CA, USA). RNA Purified Total RNA Extraction Kit (RP1201) and super M-MLV reverse transcriptase (RP6502) were purchased from BioTeke (Beijing, China). Total Protein Extraction Kit (P0027) was purchased from Beyotime (Shanghai, China). MTT (M-2128) was purchased from Sigma (USA).

Cells and animals

NSCLC cell lines HCC827 (7-1150) and A549 (7-1006) were obtained from Chi Scientific (MA, USA). Cells were maintained in RPMI 1640 medium (Invitrogen, Carlsbad, CA, USA) supplemented with 10% heat-inactivated fetal bovine serum (FBS) in a 37°C, 5% CO_2 atmosphere. BALB/c mice were provided by Changsheng Biotechnology (Liaoning, China) and housed in cages at room temperature (20°C to 25°C) under a constant humidity (55±5%) with access to food and water *ad libitum*. All the procedures on the animals were performed following the Guidelines for the Care and Use of Laboratory Animals and approved by the Institutional Animal Ethics Committee of Shandong University.

Vector construction and cell transfection

Specific shRNA oligonucleotides targeting *Src* mRNA (at 5'-GGCTCCAGATTGTCAACAA-3') and non-targeting version of shRNA were inserted into pRNA-H1.1 to form the

Indexed in: [Current Contents/Clinical Medicine] [SCI Expanded] [ISI Alerting System] [ISI Journals Master List] [Index Medicus/MEDLINE] [EMBASE/Excerpta Medica] [Chemical Abstracts/CAS]

pRNA-H1.1-shSrc vector and pRNA-h1.1-NC vector. The coding sequence for Fn14 was amplified by PCR and ligated to pcDNA3.1+ to construct the Fn14 overexpression vector (pcDNA3.1-Fn14). NSCLC cells were transfected with different vectors using Lipofectamine 2000 (Invitrogen) according to the manufacturer's instructions.

Establishment of stable *Src* knockdown cell line

HCC827 cells were divided into three groups: a) parental group, parental HCC827 cells; b) NC group, HCC827 cells transfected with the pRNA-H1.1-NC vector; and c) shSrc group, HCC827 cells transfected with the pRNA-H1.1-shSrc vector. Each group was represented by at least five replicates. After transfection, cells with stable *Src* knockdown or NC vector transfection were selected with G418 (200 μg/mL). The expression of Src in the three groups of HCC827 cells were determined by reverse transcription and real-time PCR (RT^2-PCR) and western blotting.

Overexpression of *Fn14* in *Src* knockdown cell lines

HCC827 and A549 cells with stable *Src* knockdown were further transfected with the Fn14 overexpression vector or the control pcDNA3.1+ vector: a) NC group, HCC827/A549 cells stably transfected with the pRNA-H1.1 vector; b) shSrc group, HCC827/A549 cells stably transfected with pRNA-H1.1-shSrc; c) shSrc+Vector group, *Src*-silenced HCC827/A549 cells transfected with pcDNA3.1+; and d) shSrc+Fn14 group, *Src*-silenced HCC827/A549 cells transfected with pcDNA3.1-Fn14. Forty-eight hours after transfection, the expression levels of Fn14 in different groups of cells were detected by RT^2-PCR.

In vivo metastasis assay

Eighteen BALB/c mice were randomly divided into three groups: a) control group, mice received an injection of 10^7 HCC827 cells (in 0.2 mL volume) via the tail vein; b) NC group, mice received an injection of 10^7 NC-transfected HCC827 cells via the tail vein; and c) shSrc group, mice received a tail vein injection of 10^7 *Src*-silenced HCC827 cells. The mice were raised under the same housing conditions for four weeks. Thereafter, all mice were sacrificed using the air embolism method, and the lungs were evaluated for metastatic surface nodules by gross visualization. The tumor tissues were harvested and preserved at –80°C for subsequent assays.

RT^2-PCR

The total RNA was extracted using an RNA Purified Total RNA Extraction Kit following the manufacturer's instructions. The RNA was reversely transcribed to cDNA for PCR amplification using Super M-MLV reverse transcriptase. The final RT-PCR reaction mix in 20 μL volume contained 10 μL SYBR GREEN Master Mix, 0.5 μL of each primer [Src, forward: 5'-GCTTCAACTCCTCGGACACC-3', reverse: 5'-AGCCGCTCGCCTTTCTTG-3'; β-actin (internal reference gene), forward: 5'-CTTAGTTGCGTTACACCCTTTCTTG-3', reverse: 5'-CTGTCACCTTCACCGTTCCAGTTT-3'], 1 μL cDNA template, and 8 μL Rnase-free H_2O. The reaction was performed on an Exicycler™ 96 analyzer (BIONEER, South Korea) using the following thermal cycling parameters: a denaturation step at 95°C for 10 minutes, followed by 40 cycles of amplification of 95°C for 10 seconds, 60°C for 20 seconds, and 72°C for 30 seconds. The reaction was stopped at 25°C for 5 minutes. The relative expression levels of *Src* were calculated based on the formula of $2^{-\Delta\Delta Ct}$.

Western blotting assay

Total cellular protein was extracted using the Total Protein Extraction Kit according to the manufacturer's instructions. β-actin (for cytoplasmic protein) and Histone H3 (for nuclear protein) were used as internal reference proteins. The concentrations of the protein samples were determined using the BCA method. Subsequently, 40 μg proteins from each sample was subjected to 10% sodium dodecylsulfate polyacrylamide gel electrophoresis (SDS-PAGE) at 80 V for 2.5 hours, and the proteins were then transferred onto polyvinylidene difluoride (PVDF) membranes. After being rinsed with TTBS, the membranes were blocked with skimmed milk solution for one hour. Thereafter, the membranes were incubated with the primary antibodies [Fn14 (1: 500), IκBα (1: 500), p-IκBα (1: 500), IKKβ (1: 500), p-IKKβ (1: 500), NF-κB p65 (1: 400), β-actin (1: 1,000) or Histone H3 (1: 500)] at 4°C overnight. Following four washes with TTBS, the membranes were incubated with HRP-conjugated secondary antibodies (1: 5,000) for 45 minutes at 37°C. After another six washes with TTBS, the blots were developed using the Beyo ECL Plus reagent and the images were recorded in the Gel Imaging System. The relative levels of the proteins of interest were calculated by the Gel-Pro-Analyzer (Media Cybernetics, USA).

Colony formation assay

The anchorage-independent growth capability determines the tumorigenicity of cancer cells. Thus, NSCLC cells were subjected to colony formation assay for the assessment of anchorage-independent growth. The cells were suspended in the culture media containing 10% FBS and 0.35% agarose, and then inoculated onto 35 mm plates at a density of 200 cells per plate. After culture at 37°C for two weeks, the colonies on the plates were stained with Wright-Giemsa stain for five minutes, and the number of colonies on each plate was counted using a microscope. Colony formation rate = colony number/inoculated cell number per plate ×100%.

Indexed in: [Current Contents/Clinical Medicine] [SCI Expanded] [ISI Alerting System] [ISI Journals Master List] [Index Medicus/MEDLINE] [EMBASE/Excerpta Medica] [Chemical Abstracts/CAS]

MTT assay

The viability of HCC827 cells were measured by MTT assay. Cells at the exponential growth phase were plated in 96-well plates at a density of 3×10^3/well, and cultured for 96 hours. Every 24 hours, 5 mg/mL MTT was added into the selected wells for four-hour incubation at 37°C. Thereafter, the supernatant was aspirated and 200 µL DMSO was added into each well. The cell viability was represented by the OD_{490} value which was measured using a microplate reader (ELX-800, BIOTEK, USA).

Scratch assay

The mobility of NSCLC cells after *Src* knockdown was evaluated by the scratch assay. Cells were seeded in a 24-well plate at a density of 2×10^4 cells/well, and reference points were marked to guarantee the same area of image acquisition. The cells were allowed to grow into a confluent monolayer at 37°C for 24 hours. Then the layer was scratched to form a cell-free straight line, and the debris at the edges of the scratch was removed by rinsing with PBS. Cell migration towards the midline of the scratch was recorded in reference with the reference points. Three images were captured with a phase-contrast microscope and the gap distances were measured at 0 hour, 12 hours, and 24 hours after scratching. The migration rate was defined as the percentage of gap closure and the data were analyzed with the ImageJ software (US National Institutes of Health).

Transwell assay

Then 200 µL medium containing 2×10^4 cells were plated in the upper chamber of a Transwell system (BSA-coated porous polycarbonate membrane with a pore size of 8 µm, Corning star, Cambridge, MA, USA). Each polycarbonate membrane was precoated with 40 µL Matrigel (1.5 mg mL; BD Biosciences, San Jose, CA, USA) and incubated at 37°C for two hours to form a reconstituted basement membrane. Cells were allowed to migrate through the Matrigel and the porous membrane for four hours at 37°C. After removing the cells on the upper surface of the membrane, the cells on the lower surfaces of the membrane were stained with 1% (w/v) crystal violet for 30 seconds and numbered with the Image-Pro Plus 6.0 software (Nikon).

Immunofluorescent detection

Nuclear translocation of NF-κB p65 was detected by immunofluorescent staining. Cells were seeded in 14-well chambers. After having grown into a monolayer, the cells were fixed with 4% paraformaldehyde for 15 minutes and permeabilized with 0.5% Triton X-100 for 30 minutes. Then the cells were blocked with 10% goat serum for 15 minutes, and incubated with a primary rabbit polyclonal antibody against NF-κB p65 (1: 200) overnight at 4°C. The cy3-labeled secondary antibody (1: 100) was added onto the cells and incubated for one hour. After being washed with PBS, the cells were stained with 4,6-diamino-2-phenyl indole (DAPI) for five minutes at room temperature. Following another three cycles of five-minute washes with PBS, the cells were imaged with a fluorescent microscope at 400x magnification.

Hematoxylin and eosin (H&E) staining

The histological changes in the lungs from different groups of mice were examined by hematoxylin and eosin (H&E) staining. The tissues were fixed with 4% formaldehyde, dehydrated in ascending concentrations of alcohol and permeated with dimethylbenzene. Subsequently, the tissues were embedded in paraffin, sectioned and stained with H&E. The stained sections were observed under a microscope at 100x magnification. Following H&E staining, the nuclei were stained blue and the cytoplasm was stained red.

Statistical analysis

The data were expressed as mean ±SD, and each assay was performed with at least three replicates. Multiple comparisons were performed using ANOVA followed by post-hoc Duncan test in order to control the type I error. Significance was accepted when the two-tailed p value was smaller than 0.05. All the statistical analyses and graph plotting were conducted using GraphPad Prism version 6.01 for windows (GraphPad Software).

Results

Knockdown of *Src* suppressed the viability and anchorage independent growth of HCC827 cells

As shown in Figure 1A, 1B, the expression of *Src* was inhibited in HCC827 cells stably transfected with pRNA-H1.1-shSrc. The cell viability represented by OD_{490} readings increased with time in all three groups of cells (Figure 1C). However, after 48 hours of the assay, the difference in the OD_{490} value between the shSrc group and the control or the NC group were statistically significant ($p<0.05$). The results implied a key role of Src in the proliferation of NSCLC cells. Moreover, the anchorage independent growth ability of tumor cells was critical to the process of tumorigenesis. Here, knockdown of *Src* decreased the colony number in the shSrc group, and the differences between the shSrc group and the other two groups were statistically significant (Figure 1D). These results demonstrated that Src plays an important role in the tumorigenicity and growth of NSCLC cells.

Indexed in: [Current Contents/Clinical Medicine] [SCI Expanded] [ISI Alerting System] [ISI Journals Master List] [Index Medicus/MEDLINE] [EMBASE/Excerpta Medica] [Chemical Abstracts/CAS]

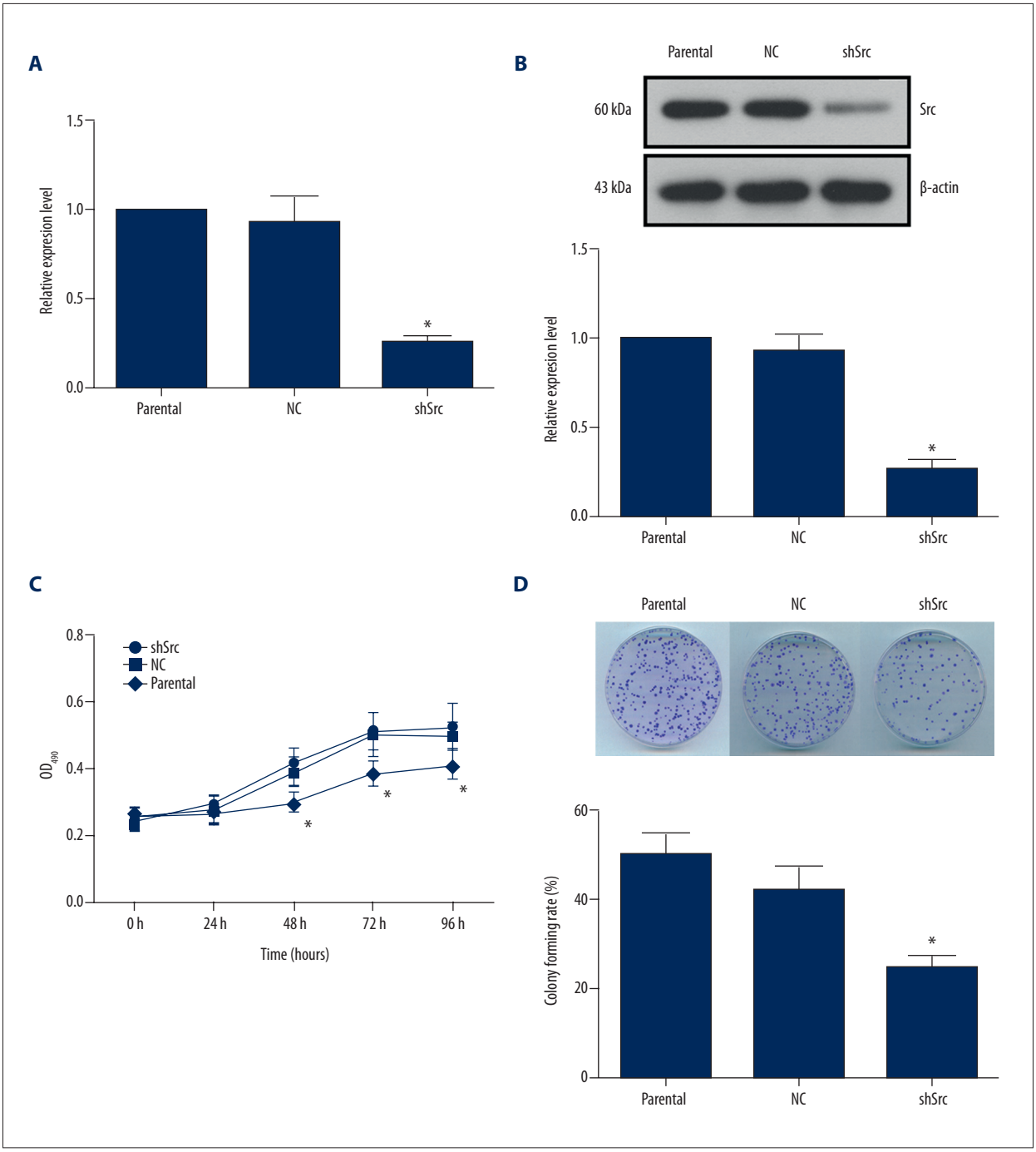

Figure 1. Knockdown of *Src* decreased cell viability and colony formation in HCC827 cells. (**A**) RT²-PCR validation of *Src* expression in HCC827 cells with or without *Src* knockdown. (**B**) Representative images and quantitative analysis of western blotting validation of Src expression. (**C**) Quantitative analysis of the effect of *Src* knockdown on cell viability. Silencing of *Src* significantly decreased the OD_{490} value in the shSrc group after 48 hours of the assay. (**D**) Representative images and quantitative analysis of anchorage independent growth of HCC827 cells with or without *Src* knockdown. Silencing of *Src* decreased the colony number formed in the shSrc group. * $p<0.05$ versus parental group.

Indexed in: [Current Contents/Clinical Medicine] [SCI Expanded] [ISI Alerting System] [ISI Journals Master List] [Index Medicus/MEDLINE] [EMBASE/Excerpta Medica] [Chemical Abstracts/CAS]

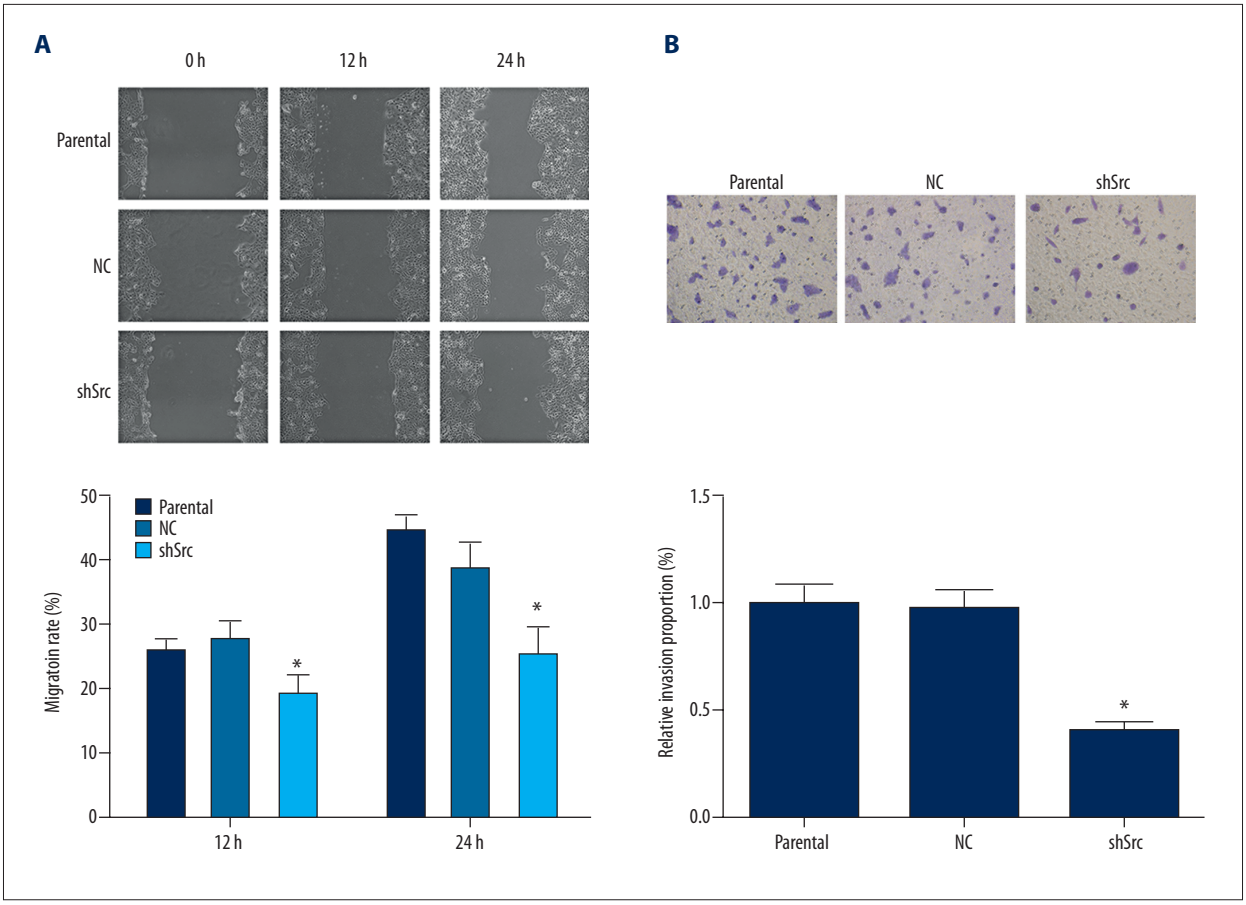

Figure 2. Knockdown of *Src* impaired the migration and invasion abilities in HCC827 cells. (**A**) Representative images and quantitative analysis of the effect of *Src* knockdown on the migration of HCC827 cells, as assessed by the scratch assay. For both recording time points, cells with *Src* knockdown showed a delayed closure rate when compared with cells in the parental group. (**B**) Representative images and quantitative analysis of the Transwell assay results for the assessment of the effect of *Src* knockdown on the invasion of HCC827 cells. Knockdown of *Src* resulted in a lower number of HCC827 cells penetrating the Matrigel-coated polycarbonate membrane. * $p<0.05$ versus parental group. Magnification, 400×.

Knockdown of *Src* inhibited migration and invasion of HCC827 cells

The high rate of metastasis in NSCLC is a key contributor to the poor prognosis of NSCLC patients. Thus, the function of Src in the migration and invasion abilities of HCC827 cells was studied. As demonstrated by the scratch assay, knockdown of *Src* in HCC827 cells led to delayed gap closure compared with parental HCC827 cells (Figure 2A). In addition, knockdown of *Src* reduced the invasiveness of HCC827 cells, as indicated by a significantly lower proportion of cells penetrating the Matrigel-coated membrane after *Src* knockdown (Figure 2B). Taken together, Src not only contributed to proliferation, but also promoted metastasis of NSCLC cells.

Overexpression of Fn14 restored the metastatic potential and activation of NF-κB signaling in *Src*-silenced NSCLC cells

Previous evidence suggests a potential association between Src and Fn14-mediated NF-κB signaling [13,15,16]. To verify the hypothesis on the Src/Fn14/NF-κB axis in NSCLC, the activation of the signaling molecules involved in the NF-κB pathway was detected by western blotting and immunofluorescent staining. Knockdown of *Src* in HCC827 cells resulted in decreased levels of Fn14, p-IκBα, p-IKKβ, and nuclear NF-κB p65 as well as an increased level of IκBα (Figure 3A), implying the blockade of Fn14-mediated NF-κB signaling. Moreover, inhibited nuclear translocation of NF-κB p65 in *Src*-silenced cells was further validated by immunofluorescent detection (Figure 3B). Generally, inhibition of NF-κB signaling would lead to reduced aggressiveness in NSCLC cells [15–17]. In line with the previous findings, suppression of Fn14-mediated NF-κB signaling

Indexed in: [Current Contents/Clinical Medicine] [SCI Expanded] [ISI Alerting System] [ISI Journals Master List] [Index Medicus/MEDLINE] [EMBASE/Excerpta Medica] [Chemical Abstracts/CAS]

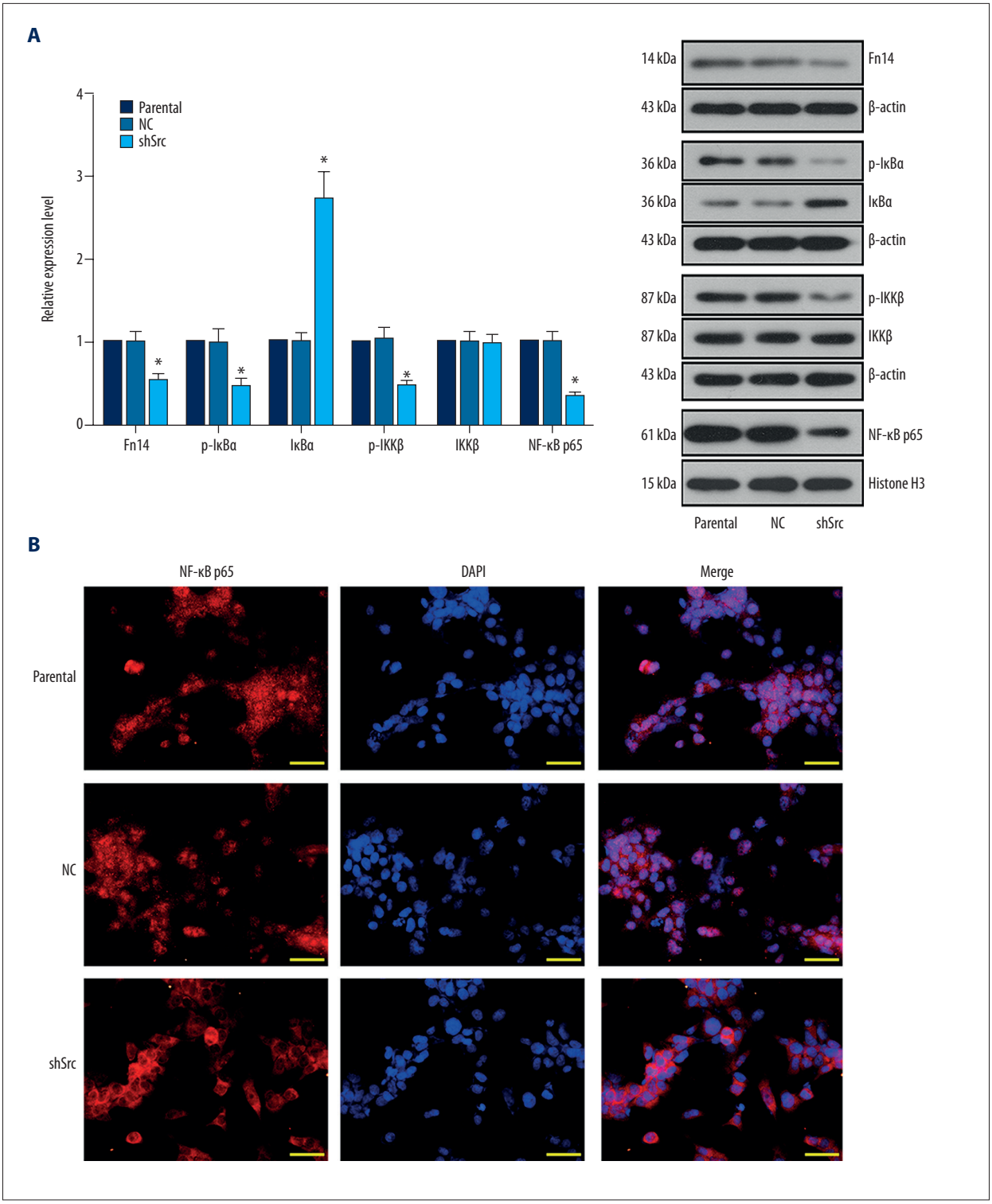

Figure 3. Knockdown of *Src* downregulated the expression of Fn14 and reduced the activation of NF-κB signaling in HCC827 cells. (**A**) Representative images and quantitative analysis of the effect of *Src* knockdown on the levels of Fn14 and the signaling molecules in the NF-κB pathway. Knockdown of *Src* induced the expression of Fn14, and elevated the levels of p-IκBα, p-IKKβ, and nuclear NF-κB p65. (**B**) Representative images of immunofluorescent detection of the effect of *Src* knockdown on the nuclear translocation of NF-κB p65. Silencing of *Src* restricted the translocation of NF-κB p65 into cell nuclei. * $p<0.05$ versus parental group. Scale bar, 50 μm.

Indexed in: [Current Contents/Clinical Medicine] [SCI Expanded] [ISI Alerting System] [ISI Journals Master List] [Index Medicus/MEDLINE] [EMBASE/Excerpta Medica] [Chemical Abstracts/CAS]

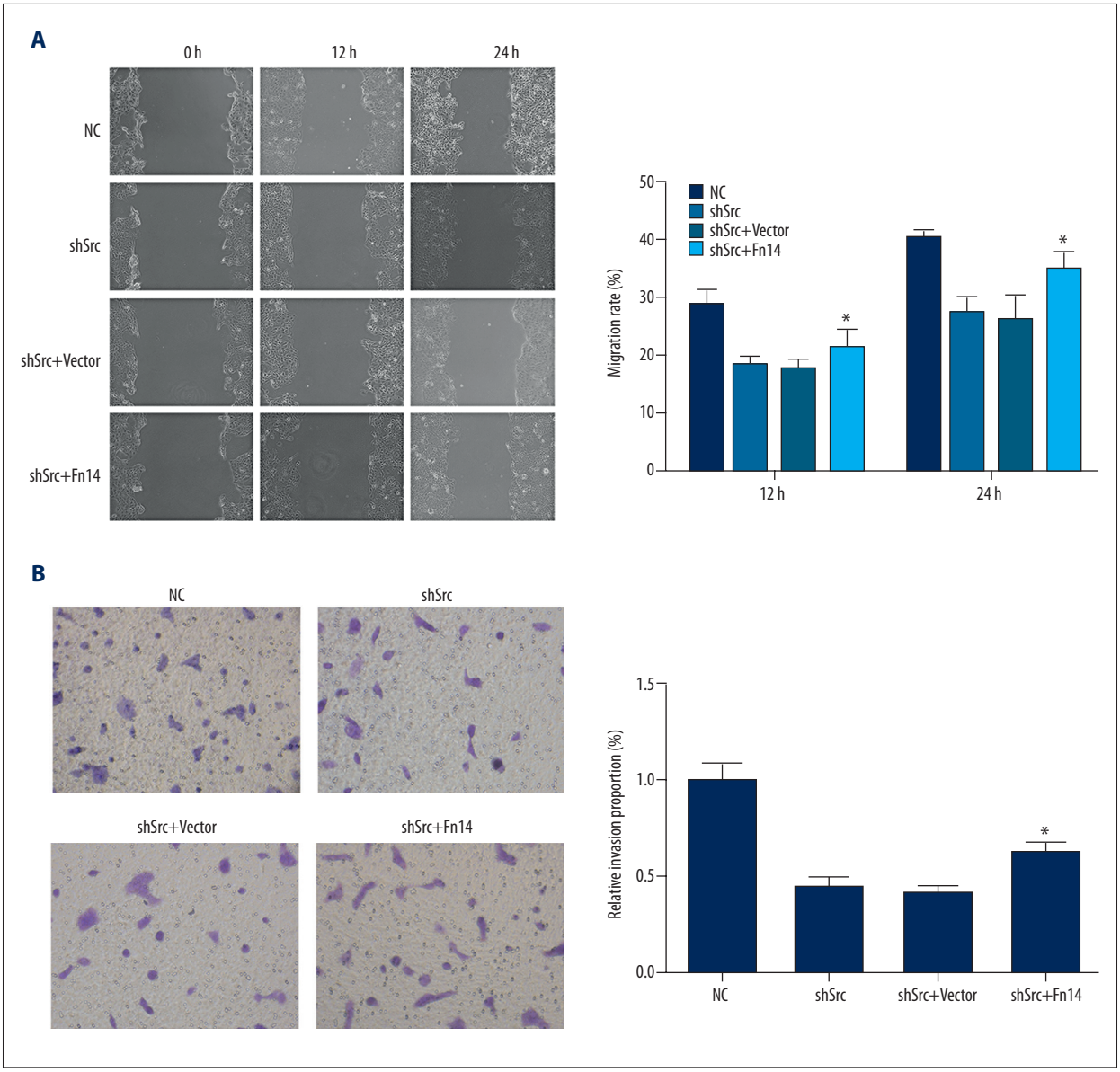

Figure 4. Overexpression of *Fn14* restored the migration and invasion abilities in *Src*-silenced HCC827 cells. (**A**) Representative images and quantitative analysis of the effect of *Fn14* overexpression on the migration of *Src*-silenced HCC827 cells. For both recording time points, the cells with *Fn14* overexpression showed a higher closure rate when compared with cells in the shSrc group. (**B**) Representative images and quantitative analysis of the effect of *Fn14* overexpression on the invasion of *Src*-silenced HCC827 cells. Overexpression of Fn14 in *Src* knockdown HCC827 cells increased the number of cells penetrating the Matrigel-coated polycarbonate membrane. * $p<0.05$ versus the shSrc group. Magnification, 400×.

by *Src* knockdown was synchronized with inhibited proliferation and metastasis of HCC827 cells (Figures 1, 2). Thus, the Src/Fn14/NF-κB axis may play an indispensable role in the cellular activities of NSCLC cells.

To confirm the aforementioned notion, *Fn14* was overexpressed in *Src*-silenced HCC827 and A549 cells by using a specific expression vector. Overexpression of *Fn14* promoted the migration and invasion of *Src*-silenced HCC827 and A549 cells (Figures 4, 5). It was also found that overexpression of Fn14 in *Src*-silenced HCC827 and A549 cells increased the levels of p-IκBα, p-IKKβ, and nuclear NF-κB p65, and decreased the level of IκBα (Figures 6, 7). The results showed that overexpression of Fn14 counteracted the inhibitory effect of *Src* knockdown on the NF-κB pathway, representing the key role of Fn14 in mediating Src-activated NF-κB pathway.

Indexed in: [Current Contents/Clinical Medicine] [SCI Expanded] [ISI Alerting System] [ISI Journals Master List] [Index Medicus/MEDLINE] [EMBASE/Excerpta Medica] [Chemical Abstracts/CAS]

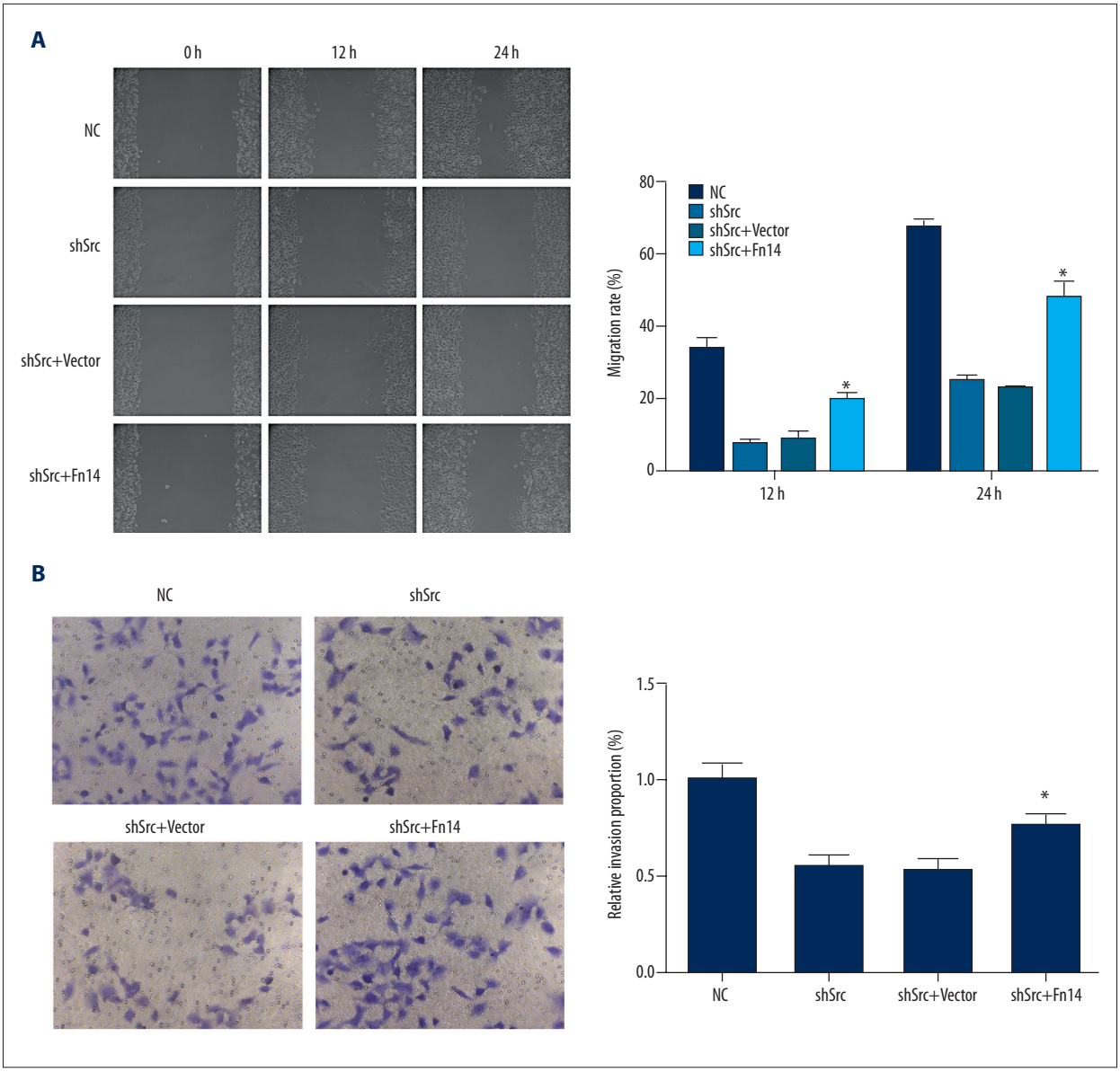

Figure 5. Overexpression of *Fn14* restored the migration and invasion abilities in *Src*-silencedA549 cells. (**A**) Representative images and quantitative analysis of the effect of *Fn14* overexpression on the migration of *Src*-silenced A549 cells. For both recording time points, cells with *Fn14* overexpression showed a higher closure rate when compared with cells in the shSrc group. (**B**) Representative images and quantitative analysis of the effect of *Fn14* overexpression on the invasion of *Src*-silenced A549 cells. Overexpression of Fn14 in *Src* knockdown A549 cells increased the number of cells penetrating the Matrigel-coated polycarbonate membrane. * $p<0.05$ versus the shSrc group. Magnification, 400×.

Knockdown of *Src* inhibited NSCLC metastasis and Fn14-mediated NF-κB signaling in mice

Based on the *in vitro* data that Src was involved in the migration and invasion of NSCLC cells, a NSCLC metastasis mouse model was employed to evaluate the effect of *Src* knockdown on NSCLC metastasis *in vivo*. As shown in Figure 8A, the number of gross lung tumors in the control group and the NC group were almost two-fold of that in the shSrc group ($p<0.05$). Similar to the *in vitro* data, the levels of Fn14 and nuclear NF-κB p65 were downregulated in the metastatic tumors derived from *Src* knockdown cells (Figure 8B). Results of the *in vivo* assay support the conclusion that Src plays a central role in NSCLC metastasis via Fn14-mediated NF-κB signaling.

Indexed in: [Current Contents/Clinical Medicine] [SCI Expanded] [ISI Alerting System] [ISI Journals Master List] [Index Medicus/MEDLINE] [EMBASE/Excerpta Medica] [Chemical Abstracts/CAS]

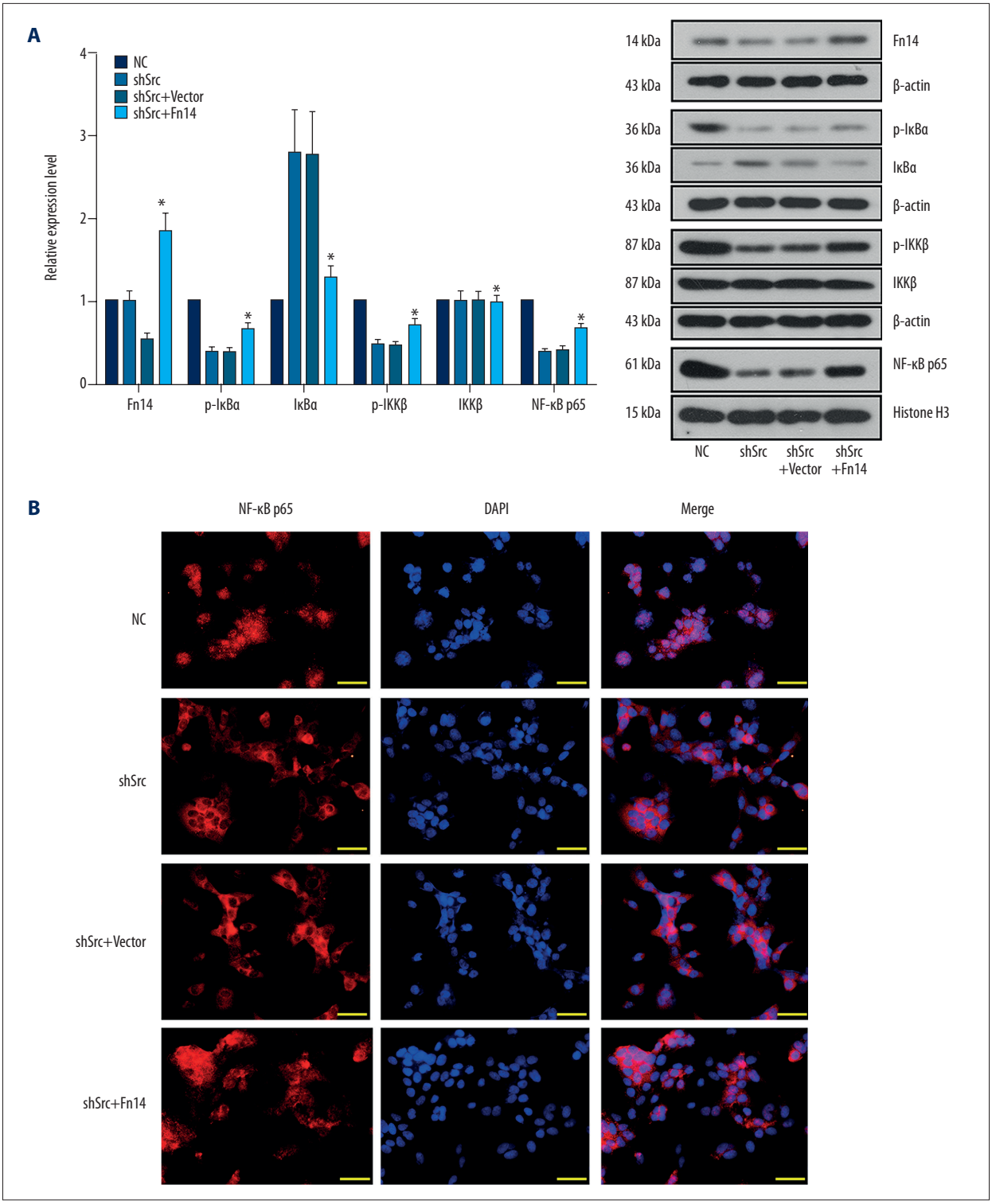

Figure 6. Overexpression of *Fn14* restored the activation of NF-κB signaling in *Src*-silenced HCC827 cells. (**A**) Representative images and quantitative analysis of the effect of *Fn14* overexpression on the expression of Fn14 and the activation of the NF-κB signaling molecules in *Src*-silenced HCC827 cells. Overexpression of *Fn14* elevated the levels of p-IκBα, p-IKKβ and nuclear NF-κB p65, representing the activation of Fn14-mediated NF-κB pathway in *Src* knockdown HCC827 cells. (**B**) Representative images of immunofluorescent detection of the effect of *Fn14* overexpression on the nuclear translocation of NF-κB p65. Overexpression of *Fn14* stimulated nuclear translocation of NF-κB p65. * $p<0.05$ versus the shSrc group. Scale bar, 50 μm.

Indexed in: [Current Contents/Clinical Medicine] [SCI Expanded] [ISI Alerting System] [ISI Journals Master List] [Index Medicus/MEDLINE] [EMBASE/Excerpta Medica] [Chemical Abstracts/CAS]

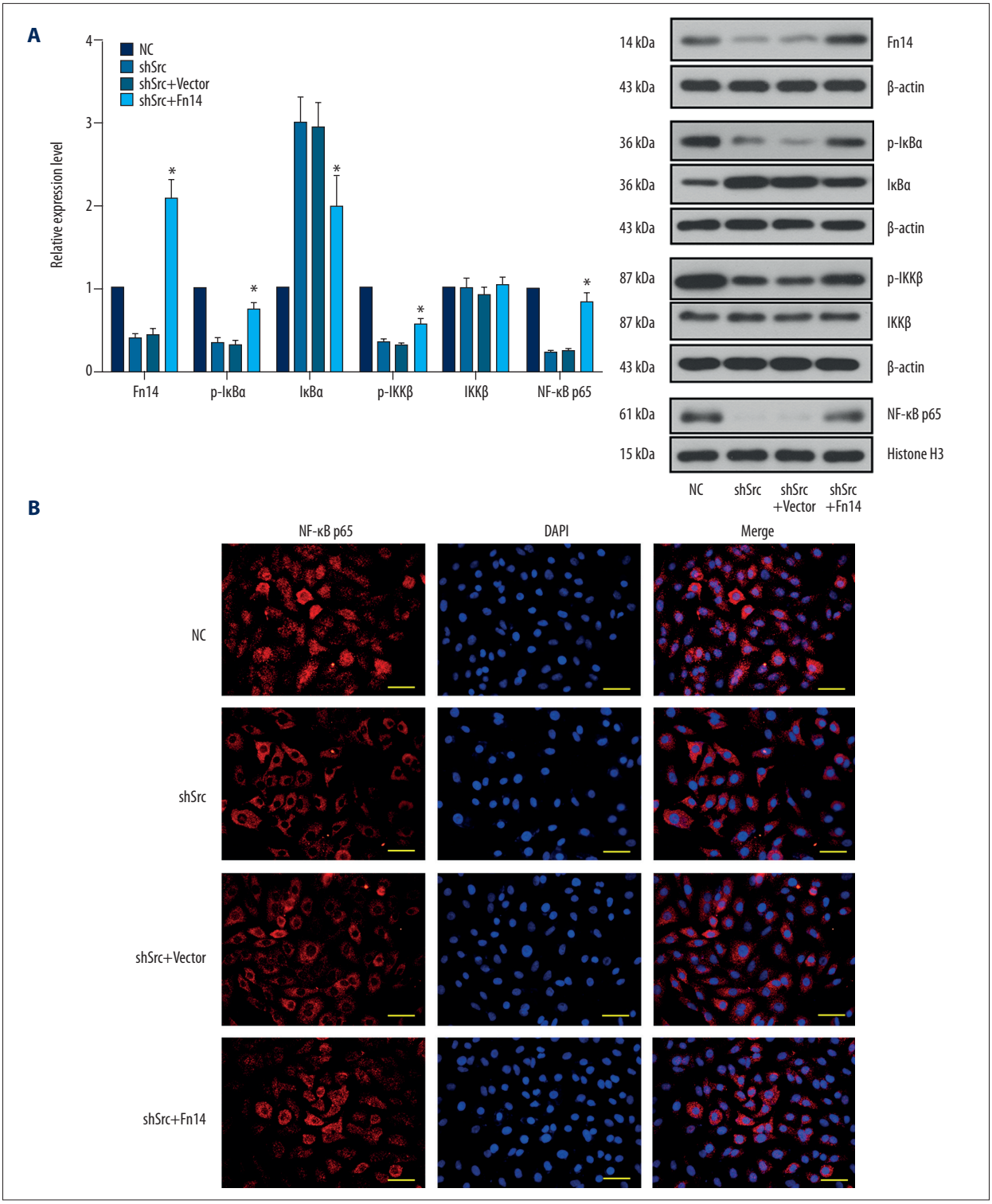

Figure 7. Overexpression of *Fn14* restored the activation of NF-κB signaling in *Src*-silenced A549 cells. (**A**) Representative images and quantitative analysis of the effect of *Fn14* overexpression on the expression of Fn14 and the activation of the NF-κB signaling molecules in *Src*-silenced A549 cells. Overexpression of *Fn14* elevated the levels of p-IκBα, p-IKKβ, and nuclear NF-κB p65, representing the activation of Fn14-mediated NF-κB pathway in *Src* knockdown A549 cells. (**B**) Representative images of immunofluorescent detection of the effect of *Fn14* overexpression on the nuclear translocation of NF-κB p65. Overexpression of *Fn14* stimulated nuclear translocation of NF-κB p65. * $p<0.05$ versus the shSrc group. Scale bar, 50 μm.

Indexed in: [Current Contents/Clinical Medicine] [SCI Expanded] [ISI Alerting System] [ISI Journals Master List] [Index Medicus/MEDLINE] [EMBASE/Excerpta Medica] [Chemical Abstracts/CAS]

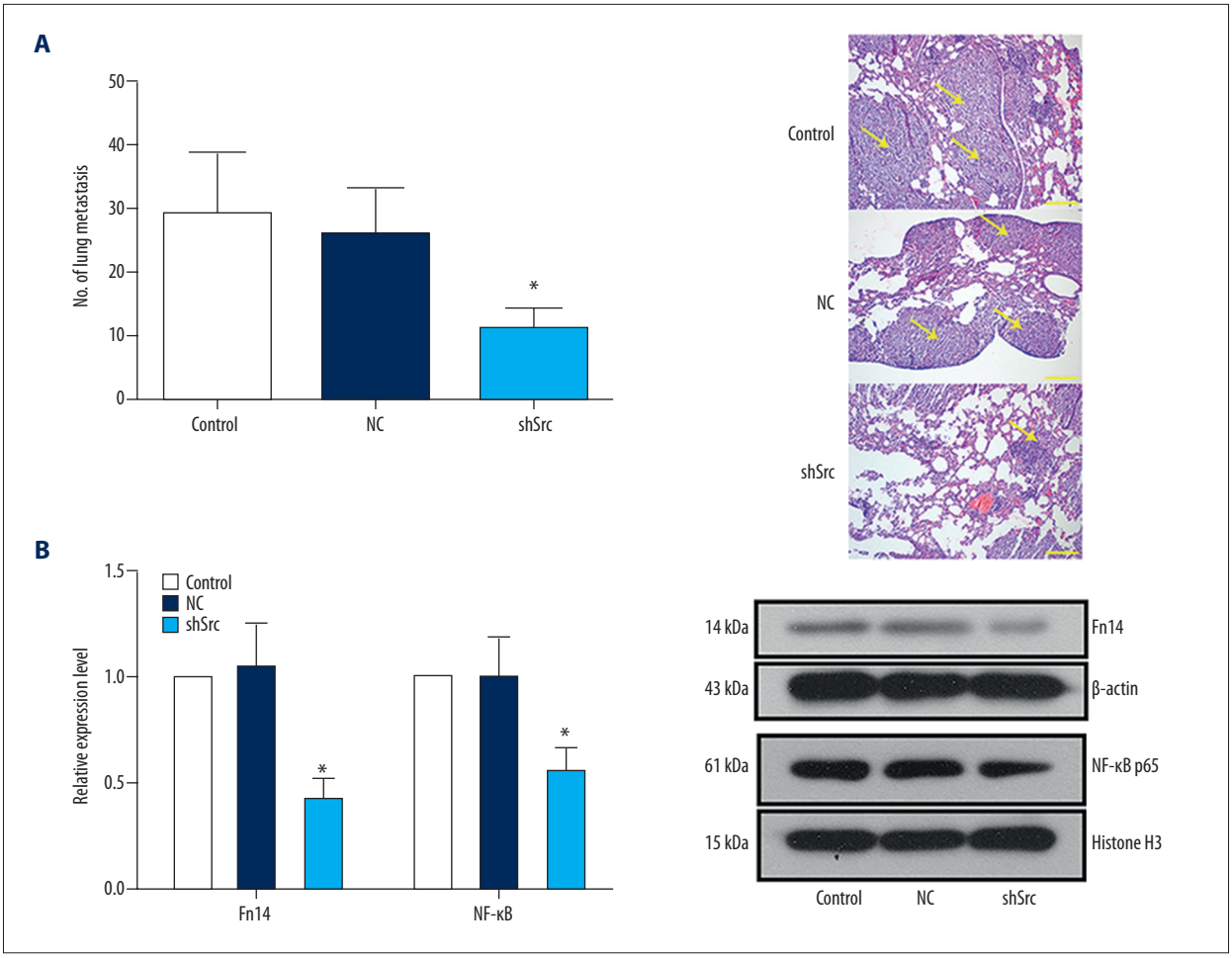

Figure 8. Knockdown of *Src* in NSCLC cells limited experimental metastases *in vivo* and inhibited Fn14-mediated NF-κB pathway. (**A**) H&E-stained lung sections and statistics of lung metastasis in BALB/c mice with tail vein injection of HCC827 cells with or without *Src* knockdown. (**B**) Representative images and quantitative analysis of the effect of *Src* knockdown on the expression of Fn14 and nuclear translocation of NF-κB p65 *in vivo*. *, $p<0.05$ versus the shSrc group. Scale bar, 200 μm. Arrows indicate metastatic tumors.

Discussion

Src kinase is emerging as a potential therapeutic target for combating the progression of NSCLC [10,11]. Inhibition of Src was previously shown to be effective in controlling the growth of lung cancer cells *in vitro* [18]. Consistently, knockdown of *Src* in the current study resulted in decreased cell proliferation and reduced metastatic potential in NSCLC cells. Moreover, as a complement to the previous reports, our data also indicated that the function of *Src* in the progression of NSCLC depended on Fn14-mediated activation of the NF-κB signaling pathway.

Aberrantly activated Src is associated with the oncogenesis of diverse types of human cancers, including those of the lung, prostate, pancreas, breast, and colon [19]. In normal physiological conditions, the activity of Src is suppressed via phosphorylation of the amino acid near the C-terminus [20]. Once the amino acid is dephosphorylated, the conformation of Src is changed, which subsequently results in the full activation of the kinase. Upregulated activity of Src initiates the signal transduction cascades involved in the emergence and progression of cancers [10]. Regarding lung cancers, increased expression of Src has been recorded in 50% of squamous cell carcinomas isolated from NSCLC patients [21]. In addition, the expression level of Src in NSCLC has been reported to be associated with the size of the solid tumor, particularly in adenocarcinomas [21]. In the current study, human lung adenocarcinoma cell line HCC827 with high expression of Src was employed as the *in vitro* model for NSCLC. It was found that knockdown of Src impaired proliferation and metastasis of HCC827 cells. In addition, silencing of Src in HCC827 cells was associated with downregulation of Fn14 and deactivation of the NF-κB pathway. According to Cheng et al., Src is an important regulator of Fn14 expression in NSCLC [13]. Moreover, in a previous report by

Indexed in: [Current Contents/Clinical Medicine] [SCI Expanded] [ISI Alerting System] [ISI Journals Master List] [Index Medicus/MEDLINE] [EMBASE/Excerpta Medica] [Chemical Abstracts/CAS]

Funakoshi-Tago et al., Src is required for IL-1-induced IKKβ activation, which in turn initiates the phosphorylation of IκBα and the activation of the NF-κB pathway [14]. In the present study, knockdown of *Src* decreased the expression of Fn14 and blocked the activation of NF-κB signaling, suggesting that Src may regulate NF-κB signaling through its downstream target, Fn14.

To explicitly uncover the relationship between Src, Fn14, and NF-κB signaling pathway, we conducted Fn14 overexpression in *Src* knockdown cells. The results showed that overexpression of Fn14 restored the cellular activities and the activation status of NF-κB signaling in *Src*-silenced NSCLC cells. These results support the notion that Src activates NF-κB signaling via Fn 14 in NSCLC cells. Fn14 is the smallest known member of the tumor necrosis factor superfamily of receptors and generally promotes tumor cell migration and invasion via activation of EGFR [22]. As for the function of Fn14 in NSCLC, Whitsett et al. indicated that TWEAK–Fn14 signaling through Mcl-1 was critical for NSCLC cell survival [16], suggesting a potential value of Fn14 in the targeted treatment of NSCLC. The modulating effect of Fn14 on NF-κB signaling has been previously demonstrated in glioma, gastric cancers, and SCLC [15]. Moreover, Li et al. reported that overexpression of Fn14 led to increased activation of NF-κB, which transactivated the downstream Bcl-xl [15]. Taken together, it can be concluded that the function of Src in the progression of NSCLC and the activation of the NF-κB pathway depends on the activity of Fn14.

Conclusions

Src plays a key role in the oncogenesis and metastasis of NSCLC. Knockdown of *Src* inhibits proliferation, migration, and invasion of human NSCLC cells and tones down NF-κB signaling. Overexpression of Fn14 in *Src*-silenced NSCLC cells rescues the cell phenotype and resumes the activation of the NF-κB pathway. Our data demonstrated the critical role of the Src/Fn14/NF-κB axis in NSCLC growth and metastasis, and the potential therapeutic value of this axis is worth further evaluation in the future.

Reference:

1. Jemal A, Bray F, Center MM: Global cancer statistics, 2011. Cancer J Clin, 2011; 58(2): 69–90
2. Wang TL, Ren YW, Wang HT et al: Association of Topoisomerase II (TOP2A) and Dual-Specificity Phosphatase 6 (DUSP6) single nucleotide polymorphisms with radiation treatment response and prognosis of lung cancer in Han Chinese. Med Sci Monit, 2018; 24: 984–93
3. Dong J, Mao Y, Li J, He J: Stair-climbing test predicts postoperative cardiopulmonary complications and hospital stay in patients with non-small cell lung cancer. Med Sci Monit, 2018; 24: 1436–14
4. Kamangar F, Dores GM, Anderson WF: Patterns of cancer incidence, mortality, and prevalence across five continents: defining priorities to reduce cancer disparities in different geographic regions of the world. J Clin Oncol, 2006; 24(14): 2137–50
5. Byers LA, Sen B, Saigal B et al: Reciprocal regulation of c-Src and STAT3 in non-small cell lung cancer. Clin Cancer Res, 2009; 15(22): 6852–61
6. Jemal A, Siegel R, Xu J, Ward E: Cancer statistics, 2010. Cancer J Clin, 2010; 60(5): 277–300
7. Wang S, Liu F, Zhu J et al: DNA repair genes ERCC1 and BRCA1 expression in non-small cell lung cancer chemotherapy drug resistance. Med Sci Monit, 2016; 22: 1999–2005
8. Johnson FM, Gallick GE: SRC family nonreceptor tyrosine kinases as molecular targets for cancer therapy. Anti-Cancer Agents Me, 2007; 7(6): 651–59
9. Patel A, Sabbineni H, Clarke A, Somanath PR: Novel roles of Src in cancer cell epithelial-to-mesenchymal transition, vascular permeability, microinvasion and metastasis. Life Sci, 2016; 157: 52–61
10. Giaccone G, Zucali PA: Src as a potential therapeutic target in non-small-cell lung cancer. Ann Oncol, 2008; 19(7): 1219–23
11. Sarries C, Haura EB, Roig B et al: Pharmacogenomic strategies for developing customized chemotherapy in non-small cell lung cancer. Pharmacogenomics, 2002; 3(6): 763–80
12. Masaki T, Igarashi K, Tokuda M et al: pp60 c-src activation in lung adenocarcinoma. Eur J Cancer, 2003; 39(10): 1447–55
13. Cheng E, Whitsett TG, Tran NL, Winkles JA: The TWEAK receptor Fn14 is an Src-inducible protein and a positive regulator of Src-driven cell invasion. Mol Cancer Res, 2014; 13(3): 575–83
14. Funakoshi-Tago M, Tago K, Andoh K et al: Functional role of c-Src in IL-1-induced NF-κB activation: c-Src is a component of the IKK complex. J Biochem, 2005; 137(2): 189–97
15. Li X, Zhu W, Chen Z et al: Fibroblast growth factor-inducible 14 regulates cell growth and multidrug resistance of small-cell lung cancer through the nuclear factor-κB pathway. Anti-cancer Drug, 2014; 25(10): 1152–64
16. Whitsett TG, Mathews IT, Cardone MH et al: Mcl-1 mediates TWEAK/Fn14-induced non-small cell lung cancer survival and therapeutic response. Mol Cancer Res, 2014; 12(4): 550–59
17. Li J, Lau GK, Chen L et al: Interleukin 17A promotes hepatocellular carcinoma metastasis via NF-κB induced matrix metalloproteinases 2 and 9 expression. Plos One, 2011; 6(7): e21816
18. Ceppi P, Papotti M, Monica V et al: Effects of Src kinase inhibition induced by dasatinib in non-small cell lung cancer cell lines treated with cisplatin. Mol Cancer Res, 2009; 8(11): 3066–74
19. Summy JM, Gallick GE: Src family kinases in tumor progression and metastasis. Cancer Metast Rev, 2003; 22(4): 337–58
20. Macauley A, Cooper JA: Structural differences between repressed and derepressed forms of p60c-src. Mol Cell Biol, 1989; 9(6): 2648–56
21. Mazurenko NN, Kogan EA, Zborovskaya IB, Kisseljov FL: Expression of pp60c-src in human small cell and non-small cell lung carcinomas. Eur J Cancer, 1992; 28(2–3): 372–77
22. Winkles JA: The TWEAK-Fn14 cytokine-receptor axis: Discovery, biology and therapeutic targeting. Nat Rev Drug Discov, 2008; 7(5): 411–25

Indexed in: [Current Contents/Clinical Medicine] [SCI Expanded] [ISI Alerting System] [ISI Journals Master List] [Index Medicus/MEDLINE] [EMBASE/Excerpta Medica] [Chemical Abstracts/CAS]